Confinement of enhanced field investigated by tip-sample gap regulation in tapping-mode tip-enhanced Raman microscopy

Taka-aki Yano[a] and Taro Ichimura[a]
Department of Applied Physics, Osaka University, Suita, Osaka 565-0871, Japan

Atsushi Taguchi and Norihiko Hayazawa[a]
RIKEN, Wako, Saitama 351-0198, Japan

Prabhat Verma[a] and Yasushi Inouye[a),b)]
Graduate School of Frontier Biosciences, Osaka University, Suita, Osaka 565-0871, Japan

Satoshi Kawata[a),c)]
Department of Applied Physics, Osaka University, Suita, Osaka 565-0871, Japan

(Received 3 July 2007; accepted 26 August 2007; published online 17 September 2007)

The authors developed a tip-enhanced near field Raman microscope that can precisely regulate longitudinal distance between a metallic tip and sample molecules. This was done by employing a time-gated photoncounting scheme that enabled us to observe exponentially decaying near field Raman intensity with the tip-sample distance. The exponential decay shows a characteristic of the enhanced field generated by the localization of the surface plasmon polaritons near the tip apex. This microscope was applied to evaluate metal-coated tips and also to investigate confinement of the field generated at a gap between two metal nanostructures from the decay curves. © *2007 American Institute of Physics*. [DOI: 10.1063/1.2785115]

Tip-enhanced near field microscopy has allowed nanoscale observation and imaging of materials with a spatial resolution down to about 10 nm.[1,2] A sharp metallic tip plays an important role in the localized field enhancement which is attributed to surface plasmon polaritons (SPPs) locally confined in the close vicinity of the tip apex.[3] The localized field excited at the tip apex are usually characterized from the scattering spectra under white light illumination, which exhibits the plasmon resonance of the metallic tip.[4] An alternative method of characterizing the field at the tip end could be directly probing the spatial confinement of the enhanced field through the optical interactions between the tip and the sample material, which needs a precise control of the longitudinal distance (along the tip axis) between the tip and the sample. This can be done by measuring a precise distance dependence of tip-enhanced Raman scattering[5,6] (TERS) or tip-enhanced fluorescence.[7–9] The former, however, has an advantage as Raman scattering does not suffer from any quenching of signal near a metal surface. The distance dependence of TERS has been previously reported, where the TERS system utilized a shear-force controlled metallic tip. In the shear-force based atomic force microscope (AFM) system, the tip is attached to a tuning fork that vibrates laterally parallel to the sample surface at its resonant frequency maintaining certain distance from the sample surface.[10] In this letter, in order to precisely control the tip-sample distance, we developed a tip-enhanced near field Raman microscope using a tapping-mode AFM, in which the metallic tip vibrated longitudinally perpendicular to the sample surface and was in cyclic contact with the sample surface during its sinusoidal oscillation. The distance dependent Raman signal was measured by setting narrow time gates and by precisely controlling time delay of the gates. The Raman signal exhibited an exponential decay with the tip-sample distance, which indicated an exponential decay of the enhanced evanescent field confined at the apex of the metallic tip. Since the field confinement as well as the enhancement depend significantly on the size and the shape of the tip apex, we demonstrate that the quality of the metallic tips can be evaluated by measuring the distance dependence of the confined fields at the tip apexes, even though the scanning electron microscope (SEM) images of the tip apexes may not show any significant difference on the surface morphology. Furthermore, we demonstrate that this technique can also be used to evaluate the confinement of the enhanced field at a gap between two metallic nanostructures by precisely regulating the gap between a metal tip and a metal substrate.

Figure 1(a) shows a schematic of the time-gated tip-enhanced Raman microscopic system. A similar time-gated technique was previously utilized for the measurement of fluorescence imaging.[11] Our system is based on an inverted optical microscope combined with a tapping-mode AFM that longitudinally vibrated a metal-coated cantilever tip at a certain frequency over sample molecules dispersed on a glass

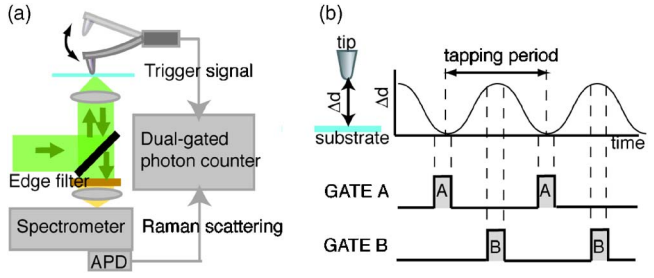

FIG. 1. (Color online) (a) Experimental setup for a tip-enhanced near field Raman system using tapping-mode AFM. (b) Schematic of the dual-gating photon counting scheme.

[a)]Also at: CREST, Japan Corporation of Science and Technology (JST), Kawaguchi 322-0012, Japan.
[b)]Electronic mail: ya-inoue@ap.eng.osaka-u.ac.jp
[c)]Also at: RIKEN, Wako, Saitama 351-0198, Japan.

substrate. The AFM cantilever, which was made of silicon, was precoated with silver nanoaggregates produced by the mirror reaction method.[12] Raman scattering from the sample was excited by a frequency-doubled $Nd:YVO_4$ laser ($\lambda = 532$ nm) which was radially polarized with the use of a four-divided half-waveplates in order to efficiently confine the incident field at the tip apex.[13] The excited Raman scattering was detected by an avalanche photodiode through a monochromator. Raman scattering from a certain vibrational mode was captured by a dual-gated photon counter while the gates were triggered synchronously with the longitudinal vibration of the AFM cantilever tip. Figure 1(b) shows a schematic of dual-gated photon counting process that was utilized to measure the dependence of tip-enhanced Raman scattering on the longitudinal distance (Δd) between a tip and a sample. The sinusoidal signal (upper curve in the figure) from AFM controller corresponds to the longitudinal vibration of the tip at a certain frequency. The two gates (gate A and gate B) were independently opened within the tapping period. The time delay of gate A was set at the time when the tip was closest to the sample surface by adjusting the gate delay. On the other hand, the time delay of gate B was set at the time when the tip was farthest from the sample surface. Therefore, the Raman intensity (I_A) measured through gate A included both near field and far field Raman components from the sample, while the intensity (I_B) measured through gate B included only the far field Raman scattering component. Finally, the output signal was obtained by subtracting I_B from I_A, resulting in extraction of pure near field contribution. In addition to a complete elimination of the far field background signal, when the time delay of gate A was swept through the entire tapping period while keeping the time delay of gate B fixed, one could obtain the tip-sample distance dependence of the near field component of the tip-enhanced Raman intensity.

Single-wall carbon nanotubes (SWCNTs) were used as a sample to demonstrate the measurement of distance-dependent TERS through the dual gating technique. Bundles of SWCNTs, with height of a few nanometers, were dispersed on a glass substrate. The vibrational frequency of the silver-coated cantilever used here was 122 kHz, which corresponds to a tapping period of 8.25 μs. The tip was positioned on the SWCNTs inside the laser focus spot, and the Raman scattering of the G band (originating from the tangential stretching vibrational modes of SWCNTs) was measured at the central frequency of 1595 cm^{-1} with the spectral width of 10 cm^{-1} through the dual-gating process. The circular dots in Fig. 2(a) show the near field component of tip-enhanced Raman intensities of the G band as a function of the time delay of gate A. This measurement was performed by sweeping the time delay of gate A at intervals of 0.1 μs through the tapping period while the time delay of gate B was fixed at a position corresponding to the time when the tip was farthest from the sample surface. The widths of both gates were set to 0.1 μs. Since the gate duration is only 1.2% of the total time of one period, the effect of sinusoidal variation within each gate is negligible. As can be seen in Fig. 2(a), near field Raman enhancement was observed for the gate delay between ~2 and ~4 μs, and had a maximum value at the gate delay of 2.3 μs, which corresponded to the position when the tip was closest to (i.e., in contact with) the SWCNTs. On the other hand, shown by squared dots in Fig. 2(a), when the monochromator detection

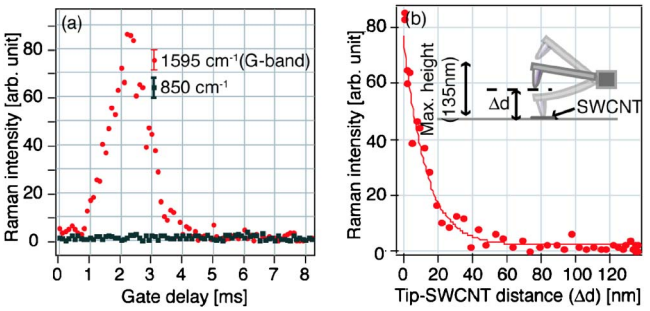

FIG. 2. (Color online) (a) Tip-enhanced near field Raman intensity of SWCNTs measured while scanning one of two gates through the entire tapping period (spherical dots: a vibrational frequency of the G band at 1595 cm^{-1}; squared dots: no vibrational frequency at 850 cm^{-1}). (b) Dependence of tip-SWCNTs distance on tip-enhanced near field Raman intensity of the G band represented from (a).

frequency was set to detect a frequency around 850 cm^{-1}, which did not correspond to any Raman mode of SWCNT, no signal enhancement was observed. This shows that the background signal was not affected by the tip-sample distance. Hence, the Raman intensity depicted with the circular dots exhibits pure near field Raman contribution from the sample existing in the vicinity of the tip. Considering the sizes of the tip apex and the focus spot of laser, the enhancement factor of the Raman scattering intensity per unit area for the G band was estimated to be about 2200.

Figure 2(b) represents the near-field Raman intensity of the G band measured from the SWCNT sample as a function of the tip-sample distance. The distance was obtained by converting the gate delay with the sinusoidal correlation. The maximum tip-sample distance was experimentally measured by using the typical method of force curve in the tapping-mode AFM operation,[14] and was found to be 135 nm. As seen in Fig. 2(b), the near field Raman intensity shows a good agreement with least square exponential fit. The decay length ($1/e$) estimated from the fit was 12 nm, which represents a measure of the longitudinal confinement of the enhanced field at the tip apex. By measuring the decay curves at different sample positions with the same tip, it was confirmed that there was no noticeable difference of their decay lengths. This result indicates that the decay curves are determined by the tip itself rather than the sample.

This technique could be very useful for evaluating the metal-coated tips since the surface roughness of the tips, originating from the shapes and the distribution of the nanoscaled silver grains, can significantly affect the decay length, even though this minor difference on the surface roughness is undetectable in SEM images of the tip apex. Figure 3(a) shows the distance dependence of near field Raman intensity of the same sample measured with a different silver-coated tips (tip A) under the same experimental conditions, as before. A comparison with the decay curve measured with the previous silver tip (tip B) as displayed once again in Fig. 3(b), shows a clear difference in the decay lengths of the two tips. We have often observed that even if the two tips, prepared under the same experimental conditions, do not show significant difference in surface morphology in SEM images, they still have significant difference in the local confinement of evanescent field at their apexes. The decay length of tip A was estimated to be 23 nm, which was 11 nm larger than that of tip B. The origin of this difference can be explained by a minor difference on the surface roughness at the apexes of

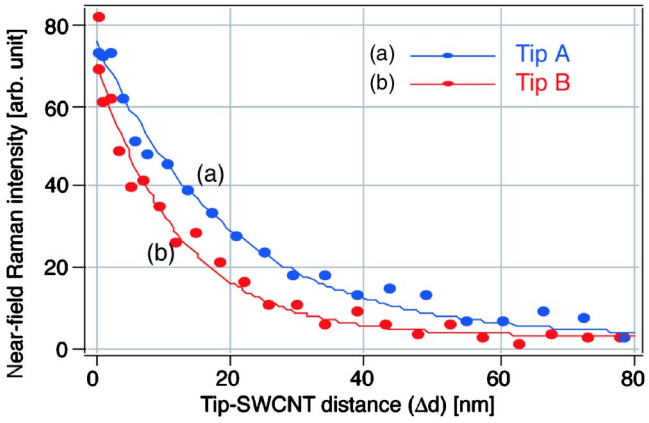

FIG. 3. (Color online) [(a) and (b)] Tip-SWCNTs distance dependent Raman intensities of the *G*-band which were measured with different silver tips (tip A and tip B). Both of the tips were prepared by the mirror reaction method under same chemical conditions.

the two tips. This roughness could be too small to be topologically discriminated; however, it affects the decay curves of Raman intensity. Therefore, this technique will enable us to evaluate the metal coating on the tip apex from the decay curves, resulting in the optimization of metallic tips for tip-enhanced Raman spectroscopy.

Finally, the tapping-mode tip-enhanced Raman system using the dual gating scheme was applied to probe the confined field generated at the gap between two metal nanostructures. The gap configuration was realized by sandwiching sample molecules between a silver tip and a silver substrate. The tip was then moved away in a controlled manner so that the effect of gap length on the enhanced Raman scattering could be measured. The silver layer was prepared by coating a glass substrate with an 8-nm-thick silver film, on which a monolayer of 4-aminothiophenol (4-ATP) molecules was self-assembled. Figure 4(a) shows gap-distance-dependent Raman intensity of 7*a*-type vibrational mode (C–S stretching mode) of 4-ATP at 1076 cm^{-1} which does not provide noticeable chemical enhancement.[15] By utilizing the same silver coated tip, the distance-dependent Raman intensity was measured when the sample molecules were dispersed either on a silver coated glass substrate or on a glass substrate

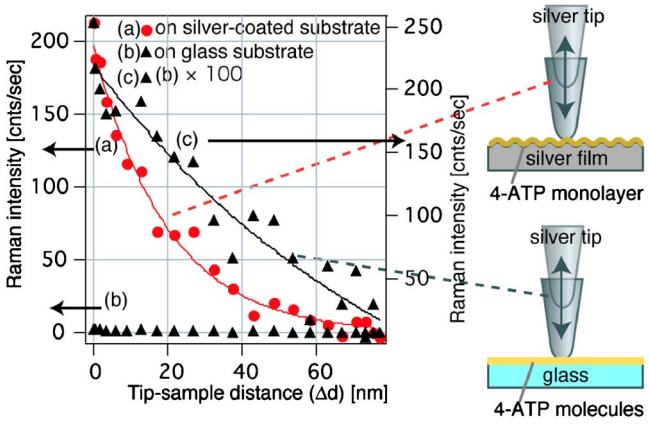

FIG. 4. (Color online) Distance dependent Raman intensities of a vibrational mode of 4-ATP at 1076 cm^{-1} which were measured on (a) silver-coated substrate and (b) nonsilver-coated substrate with the use of the same silver tip. The data of (b) are presented with a 100 times larger scale in (c) for a better comparison of the decay lengths.

without silver coating. The decay length for 4-ATP on the silver coated substrate was estimated to be 20 nm, which was 18 nm shorter than that for 4-ATP measured on glass substrate without silver coating, as shown in Fig. 4(b). Due to the overall higher enhancement of Raman scattering for the gap configuration than that for a nongap configuration, the data in Fig. 4(b) are much weaker than those in Fig. 4(a). For a better comparison of the decay lengths, the same data of Fig. 4(b) are presented in Fig. 4(c) with a 100 times higher scale. This result verified the theoretically well-known characteristic of field confinement at the gap between two metal nanostructures,[16] which showed that the gap configuration confines the enhanced field much strongly into a smaller region than the nongap configuration. As the decay length and the maximum intensity enhancement at the gap depend on the metal specie, the probing wavelength and the metal structure (size and shape), experimental evaluation of these dependencies by measuring the gap-length-dependent enhanced Raman scattering enables us to improve spatial resolution and sensitivity of the tip-enhanced Raman microscope.

While the electromagnetic interaction of the tip with the sample materials was mainly addressed in this letter, the tip-enhanced Raman microscope operating in tapping mode can also provide significant distance dependent information on the chemical[17] and mechanical[18] interactions between the sample and the tip. Apart from the changes in intensities, the chemical and mechanical interactions can show frequency shifts, enabling us to probe the dynamics of the interactions. The shifts due to mechanical effects under the usual contact mode AFM operation are within a few wavenumbers,[18] hence our present results obtained with a spectral width of 10 cm^{-1} are not affected by mechanical interactions. The chemical effects, on the other hand, can provide larger shifts. However, in the present experiments, we have avoided the chemical effects by choosing suitable samples.

[1] T. Ichimura, N. Hayazawa, M. Hashimoto, Y. Inouye, and S. Kawata, Phys. Rev. Lett. **92**, 220801 (2004).
[2] A. Hartschuh, E. J. Sanchez, X. S. Xie, and L. Novotny, Phys. Rev. Lett. **90**, 095503 (2003).
[3] Y. Inouye and S. Kawata, Opt. Lett. **19**, 159 (1994).
[4] T. Kalkbrenner, U. Hakanson, and V. Sandoghdar, Nano Lett. **4**, 2309 (2004).
[5] Y. Inouye, N. Hayazawa, K. Hayashi, Z. Sekkat, and S. Kawata, Proc. SPIE **3791**, 40 (1999).
[6] M. Stockle, Y. D. Suh, V. Deckert, and R. Zenobi, Chem. Phys. Lett. **318**, 131 (2000).
[7] E. J. Sanchez, L. Novotny, and X. S. Xie, Phys. Rev. Lett. **82**, 4014 (1999).
[8] N. Hayazawa, Y. Inouye, and S. Kawata, J. Microsc. **192**, 472 (1999).
[9] J. M. Gerton, L. A. Wade, G. A. Lessard, Z. Ma, and S. R. Quake, Phys. Rev. Lett. **93**, 180801 (2004).
[10] K. Hsu and L. A. Gheber, Rev. Sci. Instrum. **70**, 3609 (1999).
[11] T. J. Yang, G. A. Lessard, and S. R. Quake, Appl. Phys. Lett. **76**, 378 (2000).
[12] J. J. Wang, Y. Saito, D. N. Batchelder, J. Kirkham, C. Robinson, and D. A. Smith, Appl. Phys. Lett. **86**, 263111 (2005).
[13] N. Hayazawa, Y. Saito, and S. Kawata, Appl. Phys. Lett. **85**, 6239 (2004).
[14] C. Su, L. Huang, and K. Kjoller, Ultramicroscopy **100**, 233 (2004).
[15] X. Hu, T. Wang, L. Wang, and S. Dong, J. Phys. Chem. C. **111**, 6962 (2007).
[16] M. Futamata, Y. Maruyama, and M. Ishiakawa, J. Phys. Chem. B **107**, 7607 (2003).
[17] N. Hayazawa, H. Watanabe, Y. Saito, and S. Kawata, J. Chem. Phys. **125**, 244706 (2006).
[18] T. Yano, Y. Inouye, and S. Kawata, Nano Lett. **6**, 1269 (2006).